Speed-thrust Control of a Double Sided Linear Switched Reluctance Motor (DSL-SRM)

I.-A. Viorel, Member IEEE, L. Szabo, Member IEEE, Larisa Strete
Electrical Machines Dept., Technical University of Cluj-Napoca
Str. Daicoviciu, 15, 400020, Cluj-Napoca, Romania
e-mail: ioan.adrian.viorel@mae.utcluj.ro, larisa.strete@mae.utcluj.ro

***Abstract*-The speed and thrust control strategy for a double sided linear switched reluctance motor (DSL-SRM) is elaborated in the paper, based on a simplified analytical model. The strategy is defined for different motor phase supply conditions and the dynamic characteristics are calculated via computer simulation for a sample motor, in order to sustain the theoretical results.**

I. Introduction

Linear motors are a good option for low or high speed mass transfer drive systems, besides being almost the exclusive solution for high force linear actuators. Up to few years ago, linear induction and synchronous motors were prevalent in industrial applications. Nowadays, some variable reluctance linear motors, such as switched reluctance (SRM) or transverse flux reluctance (TFRM), became an attractive alternative due to the lack of windings on either the stator or mover (translator) structure.

Linear switched reluctance motors (LSRM), despite their relatively high demand for reactive power, are an attractive alternative for linear drive systems due to their three important advantages: modularity, fault tolerance and constructive simplicity. LSRMs have concentrated windings on either the stator or the mover, making them ideal for low-cost manufacturing and maintenance. Concentrated winding and totally independent phases' supply enables LSRMs to operate even with a phase shorted or open as fault-tolerant system. The LSRMs modularity means that a drive system can have as many elementary modules of three or more phases LSRM as necessary to obtain the required tangential force.

Quite many scientific works were dedicated to LSRMs construction, operation, supply and control. General hints concerning linear SRM are given in [1] and [2], while in [3] and [4] a double sided single mover LSRM is extensively presented. In [5] and [6] are detailed some interesting aspects concerning LSRM's characteristics, supply and control. From the published papers dealing with LSRM's control, two are mentioned here [7] and [8]. A simplified LSRM model is presented in [9].

In this paper, an attempt to an analytical development for LSRM control strategy is made based on a simplified mathematical model. All the developments are done considering a double sided LSRM with one mover which has low, if not zero, attraction forces. Three supply modes are discussed and for each one the basic equations are developed.

In the second Section, the structure of a three phase double sided linear switched reluctance motor (DSL-SRM) is presented. The designed sample motor main data are given too. The third Section is dedicated to the DSL-SRM simplified analytical models. Two models, one based on the variable air-gap equivalent permeance concept [6,9,10], and one using Fourier series to obtain flux linkage-current characteristics are developed, and an equivalence between these models is defined. In the fourth Section, the results obtained via two dimensions finite element method (2D-FEM) analysis are given, and thrust versus mover position characteristics, at different currents, calculated analytically, are compared with the ones computed via 2D-FEM. The phase fluxes obtained for different motor phase supply conditions are given in the fifth Section, while the dynamic characteristics calculated via computer simulation, are presented in the sixth Section. Seventh Section contains the overall conclusions.

II. DSL-SRM Structure

A double sided modular three phase linear motor construction is considered, Fig. 1. The three phase solution leads to a short module, and a single mover requires less steel laminations.

The number of modules depends on the design requirements as total traction force, overall dimensions, supply converter, etc. The mover length is imposed by the considered application, which can be a short track transfer system, for instance.

For the sake of simplicity, the calculations in the paper are carried on for two modules double sided single mover LSRM, but the results can be easily extended to motors with more than two modules.

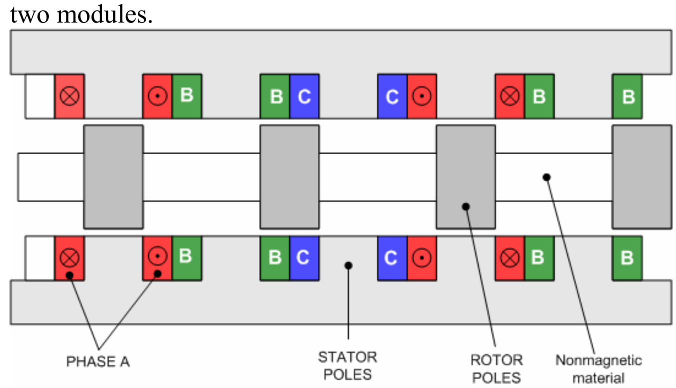

Fig. 1. Single mover double sided LSRM layout.

TABLE I
SAMPLE MOTOR MAIN DATA

	Notation	Unit	Value
Stator core width	w_S	mm	100
Stator pole pitch	τ_{pS}	mm	60
Stator pole width	w_{pS}	mm	30
Stator slot opening	w_{sS}	mm	35
Stator slot height	h_{sS}	mm	30
Stator yoke height	h_{yS}	mm	30
Mover pole pitch	τ_{yM}	mm	90
Mover pole width	w_{pM}	mm	30
Air-gap length	g	mm	1.5
Coil turns number	N_c	-	70
Rated phase current	I	A	24

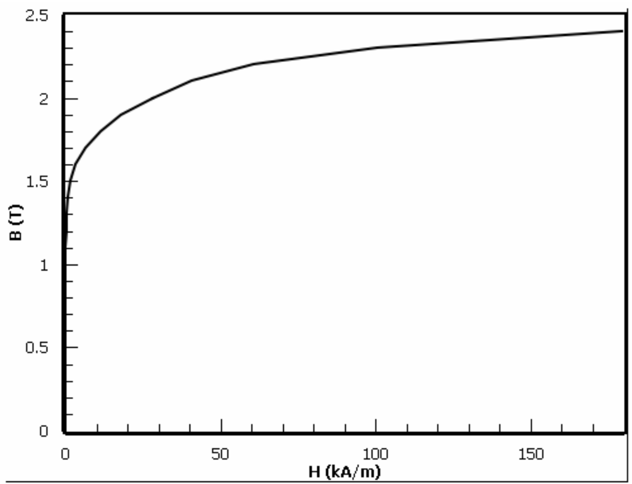

Fig. 2. Core material B = f (H) curve.

A sample three phase DSL-SRM was purposely designed. It has two modules and a simple topology, no optimization being carried out. The sample motor main data are given in Table 1. The iron core material B = f(H) curve is shown in Fig. 2.

III. DSL-SRM ANALYTICAL MODELS

Two analytical models are proposed and the equivalence between these models is defined.

One simplified model developed for LSRM, in order to define the control strategy, is based on the equivalent variable air-gap permeance method presented in [9],[10],[11],[12] where it was applied to stepper linear motor, to rotating SRM and to transverse flux reluctance motor respectively. Within the permeance model, the phase flux linkage is defined as:

$$\lambda = {N_c}^2 i \frac{\mu_0 A_p}{K_C K_S(x,i) g}\left[1 + a_g \cos(2\pi \frac{x}{\tau_{pM}})\right] \tag{1}$$

with $x \in [0, \tau_{pM}/2]$ the linear coordinate having the value zero in the aligned position. τ_{pM}, i, g, N are mover pole pitch, phase current, actual air-gap length and series number of turns per phase coil. A_p, the stator pole area is equal to the rotor pole area for the sake of simplicity. Coefficient a_g depends on the air-gap equivalent variable permeance coefficient P_{coeff} [12] and on Carter's factor K_C calculated when the slots are considered only on the mover.

The variable saturation factor K_S [12], depends on the core material and dimensions via K_{S0} and on phase current via coefficients A and B.

$$K_S = K_{S0}\left(A\cos(2\pi \frac{x}{\tau_{pM}}) + B\right) \tag{2}$$

The saturation constant K_{S0} can be calculated by:

$$K_{S0} = 1 + (1/\mu_{r0})(l_{co}/l_g) \tag{3}$$

where l_{co}, l_g are the mean length of magnetic path in the core and in the air-gap respectively, and μ_{r0} is the initial relative permeability of the core material.

The saturation factor coefficients A and B are polynomial functions of the phase current, and an estimation can be obtained through a curve fitting procedure by considering a set of saturation functions calculated for different currents.

For a given phase current value i_1, the saturation factors of aligned and unaligned mover position are calculated based on 2D-FEM analysis. The corresponding A_1 and B_1 particularly saturation function coefficients result and the same procedure is followed up for different phase current values i_2, i_3….

A set of particularly saturation functions are obtained, A_1, A_2…,B_1, B_2…and the A and B coefficients are now computed via a curve fitting procedure.

If the motor is slightly saturated, the saturation function can be considered constant

$$K_S \cong K_{S0} \tag{4}$$

The tangential force developed is calculated with the usual equation:

$$f_T = \int_0^i \frac{\partial \lambda}{\partial x} di \tag{5}$$

The flux linkage derivative function of mover position is:

$$\begin{aligned} \frac{\partial \lambda}{\partial x} &= \frac{2\pi}{\tau_{pM}} \frac{\mu_0 A_p N_c^2}{K_C g K_{S0}} \sin(2\pi \frac{x}{\tau_{pM}}) \cdot \\ &\cdot \frac{a_g A(i) - B(i)}{\left[A(i) + B(i)\cos(2\pi \frac{x}{\tau_{pM}})\right]^2} i \end{aligned} \tag{6}$$

The tangential force analytical expression can be obtained but, even if $A(i)$ and $B(i)$ are polynomials of second order, it might be quite complicated. Therefore, an approximation of the integral based on a particular case of Newton-Cotes method with the interpolating Lagrange polynomials of first degree is recommended [13].

In same references, [14] for instance, the SRM's phase flux linkage is approximated by a Fourier series with limited number of terms. If only two terms of the Fourier series are considered, then:

$$\lambda(i,x) = \lambda_0 + \lambda_1 \cos(2\pi \frac{x}{\tau_{pM}}) \tag{7}$$

$$\lambda_{al} = \lambda_0 + \lambda_{1,} \qquad \lambda_{un} = \lambda_0 - \lambda_{1,} \tag{8}$$

where λ_{al} and λ_{un} are the phase flux linkage with the mover in aligned, respectively unaligned position.

The nonlinear flux-linkage versus current characteristics in aligned mover position can be estimated via a curve fitting procedure, a ratio of polynomials being employed,

$$\lambda_{al} = \frac{i}{ai^2 + bi + c} \tag{9}$$

The flux linkage versus current characteristics in unaligned mover position is almost a linear function of phase current and can be estimated as:

$$\lambda_{un} = L_{0un} i \tag{10}$$

where L_{0un} is the unsaturated unaligned phase inductance.

The flux linkage derivative, in the case of this simplified model is:

$$\frac{\partial \lambda}{\partial x} = -\frac{2\pi}{\tau_{pM}} \sin(2\pi \frac{x}{\tau_{pM}}) \cdot \frac{1}{2}(\lambda_{al} - \lambda_{un}) \tag{11}$$

The integral I that has to be calculated to obtain the tangential force,

$$I = \int_0^i \left[\frac{i}{ai^2 + bi + c} - L_{0un} i \right] di \tag{12}$$

can be solved analytically.

From (7) (8) results:

$$\lambda(i,x) = \lambda_0 \left[1 + \frac{\lambda_1}{\lambda_0} \cos(2\pi \frac{x}{\tau_{pM}}) \right] \tag{13}$$

respectively:

$$\lambda(i,x) = N_c \frac{N_c i}{\Re_0} \left[1 + \frac{\Re_1}{\Re_0} \cos(2\pi \frac{x}{\tau_{pM}}) \right] \tag{14}$$

The equivalent reluctances $\Re_0$ and $\Re_1$ are:

$$\frac{1}{\Re_0} = 0.5 \left(\frac{1}{\Re_{al}} + \frac{1}{\Re_{un}} \right) \qquad \frac{1}{\Re_1} = 0.5 \left(\frac{1}{\Re_{al}} - \frac{1}{\Re_{un}} \right) \tag{15}$$

and the aligned $\Re_{al}$, respectively unaligned $\Re_{un}$ reluctances, which depend on phase current, are defined as:

$$\frac{1}{\Re_{al}} = \frac{\lambda_{al}}{N_c^2 i} \qquad \frac{1}{\Re_{un}} = \frac{\lambda_{un}}{N_c^2 i} \tag{16}$$

The phases flux linkage is described by the variable equivalent permeance model,

$$\lambda(i,x) = \frac{N_c^2 i}{\Re_g} \left[1 + a_g \cos(2\pi \frac{x}{\tau_{pM}}) \right] \tag{17}$$

Then the following equivalence results:

$$\Re_0 \Rightarrow \Re_g \qquad \frac{\Re_1}{\Re_0} \Rightarrow a_g \tag{18}$$

It means that, formally, the defined models are equivalent and the general results obtained by using one of them are valid in the case of the second model too.

IV. 2D-FEM Analysis

Both models require the data obtained through 2D-FEM analysis for two mover positions, aligned and unaligned. The actual designing procedure includes compulsory 2D-FEM analysis in order to obtain a suboptimal solution and to calculate the motor characteristics, mainly the tangential force versus mover position at different current characteristics.

It means that the flux linkages versus current characteristics necessary for the models calculation are always at hand and no other supplementary work is required.

The 2D-FEM analysis is preferred since the construction of the 2D structure is simpler and the results, except the leakage inductance of the end winding, are quite the same as for the ones obtained via 3D-FEM analysis, mostly for the magnetizing flux whose variation produces the tangential force.

The 2D-FEM analysis was done only for the case when both coils of the phase are supplied adequately to add their **mmf.** A symmetrical structure for phase A is considered, Fig. 3. The mover's position in Fig.3 is closer to the aligned position. For the same position in Fig. 4, the variation of the air-gap flux density is given.

As one can see, if the coils of the same phase in both modules are supplied, than practically there is no flux in the air-gap through the poles of other two phases.

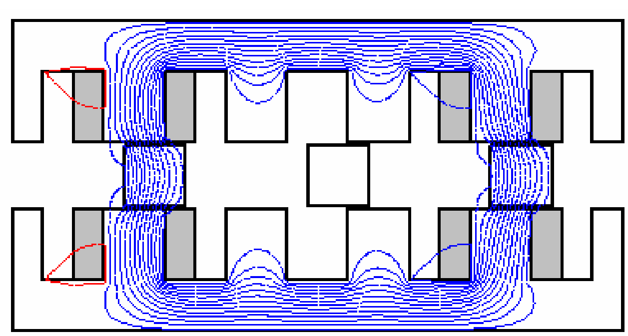

Fig. 3. Sample LSRM, flux lines, one phase supplied

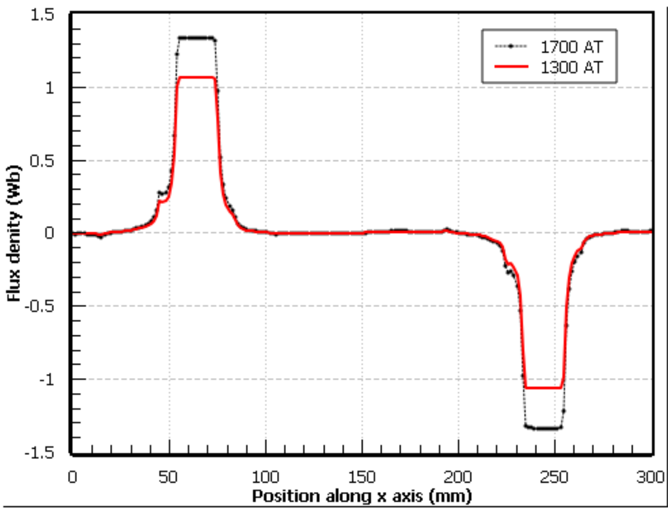

Fig. 4. Sample LSRM, air-gap flux density, one phase supplied

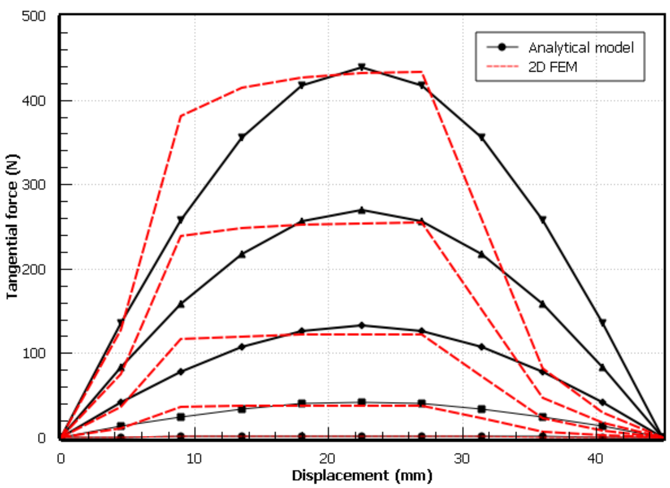

Fig. 5. Tangential force versus mover position, different phase **mmf** values

In Fig. 5 is given a comparison between the tangential force versus mover position at different values of phase **mmf** calculated via 2D-FEM analysis and respectively by using the model based on Fourier series with two terms only for phase flux-linkage. As one expects, the force calculated via analytical model has almost a sinusoidal form and is less affected by saturation, but it covers quite adequately the phenomenon

The analytical model based on variable air-gap equivalent permeance concept, which was used mostly in the designing process, is not further developed here, but, as proved already, the results should be similar.

V. Phase Flux, Different Supply Conditions

Three cases can be considered concerning the way the phase coils are supplied. The first and the most usual one, is the case when the homologous phase coils form both modules are supplied adequately. In such a case, see the field lines in Fig. 3, the flux produced by one phase **mmf** does not go through other phases poles in the air-gap.

The second case considered is that one when from two three-phase modules only one is supplied. In this case the magnetic equivalent circuit, when the core reluctances are considered through the saturation function, is presented in Fig. 6. The resulting flux equations are given in Table 2. In the third case only one module, also with three phases is considered. The magnetic equivalent circuit for this case is given in Fig. 7 while the flux equations are given in Table 2.

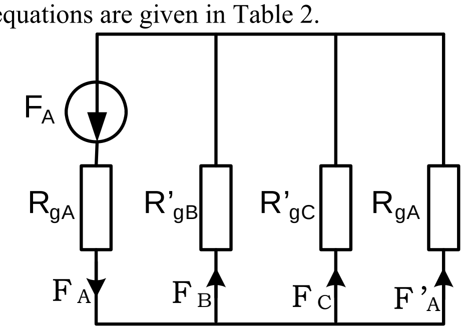

Fig. 6. Magnetic equivalent circuit, two modules

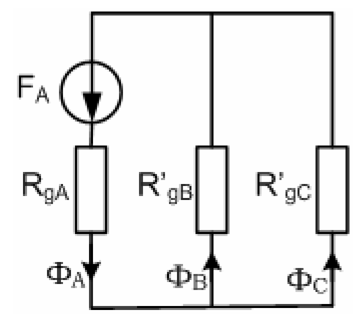

Fig. 7. Magnetic equivalent circuit, one module

TABLE II
THE PHASE FLUX EQUATIONS. THREE PHASE MOTOR, ONE COIL OF PHASE A SUPPLIED

Two modules	One module
$\Phi_A = \frac{F_A}{6\Re_0}(1+a\cos\alpha)(5-a\cos\alpha)$	$\Phi_A = \frac{F_A}{3\Re_0}(1+a\cos\alpha)(2-a\cos\alpha)$
$\Phi_B = 2\frac{F_A}{6\Re_0}(1+a\cos\alpha)(1+a\cos(\alpha+2\pi/3))$	$\Phi_B = \frac{F_A}{3\Re_0}(1+a\cos\alpha)(1+a\cos(\alpha+2\pi/3))$
$\Phi_C = 2\frac{F_A}{6\Re_0}(1+a\cos\alpha)(1+a\cos(\alpha-2\pi/3))$	$\Phi_C = \frac{F_A}{3\Re_0}(1+a\cos\alpha)(1+a\cos(\alpha-2\pi/3))$
$\Phi'_A = F_A(1+a\cos\alpha)^2/6\Re_0$	-------

The reluctances are:

$$1/\Re_{gA} = (1 + a\cos\alpha)/\Re_0$$
$$1/\Re_{gB} = (1 + a\cos(\alpha + \frac{2\pi}{3}))/\Re_0 \qquad (19)$$
$$1/\Re_{gC} = (1 + a\cos(\alpha - \frac{2\pi}{3}))/\Re_0$$
$$a = \Re_1/\Re_0, \alpha = 2\pi \cdot x/\tau_{pM}$$

In the case when DSL-SRM has only one three phase module, the phase fluxes given in Table 2, second column, the resulting traction force, for a constant phase current is:

$$f_{T11} = f_{Ti}(2\sin\alpha - 2a\sin 2\alpha) \qquad (20)$$

$$f_{Ti} = -a\frac{2\pi}{\tau_{pM}}\frac{N_C{}^2 i^2}{6\Re_0} \qquad (21)$$

The maximum value of the traction force is obtained at the mover position when the force derivative is zero,

$$\frac{\partial f_{T11}}{\partial x} = 0 \Rightarrow \alpha_{\max}\frac{2\pi}{3}, x_{\max} = \frac{\tau_{pM}}{3} \qquad (22)$$

the maximum force value being:

$$f_{T11\max} = 2.6 f_{Ti} \qquad (23)$$

In the case when DSL-SRM has two three phase modules, only one phase coil supplied, first column in Table 2 results:

$$f_{T21} = f_{Ti}(4\sin\alpha - a\sin 2\alpha) \qquad (24)$$

$$\alpha_{\max} = 1.797 rad, x_{\max} = 1.797\tau_{pM}/2\pi \qquad (25)$$

$$f_{T21\max} = 4.117 f_{Ti} \qquad (26)$$

All values are calculated for a=0.5. The variation of the tangential forces f_{T11} and f_{T21} referred to f_{ti}, function of equivalent angle α, are given in Fig. 8 for two values of the a coefficient., a = 0.3 and a = 0.5.

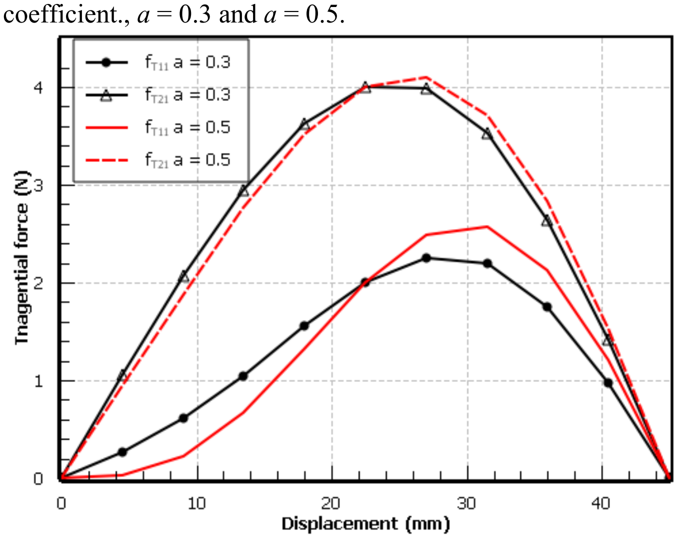

Fig.8. Referred tangential forces versus mover position

VI. DSL-SRM CONTROL

The control strategy should be based on the traction force versus mover position characteristics and its goal is to assure the maximum average traction force at a given current. Since the coefficient a is varying function of phase current, the steady state force versus mover position characteristics are giving only basics information and the control strategy should be checked via computer simulation of the entire drive system.

In the following, the SIMULINK program developed for the drive system in the case of a two three phase module DSL-SRM, both phase coils adequately supplied, and some of the obtained results are presented.

In Figure 9 a schematic view of the SIMULINK model is presented. A speed control is implemented and the results are checked for a trapezoidal speed profile. Fig. 10 displays the speed profile and the actual DSL-SRM speed which follows exactly the reference. A 30N load force is applied.

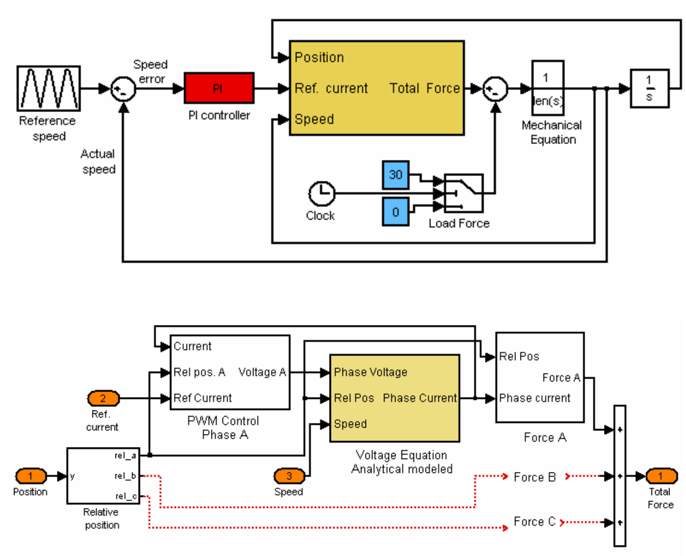

Fig. 9. Dynamic modeling using SIMULINK environment

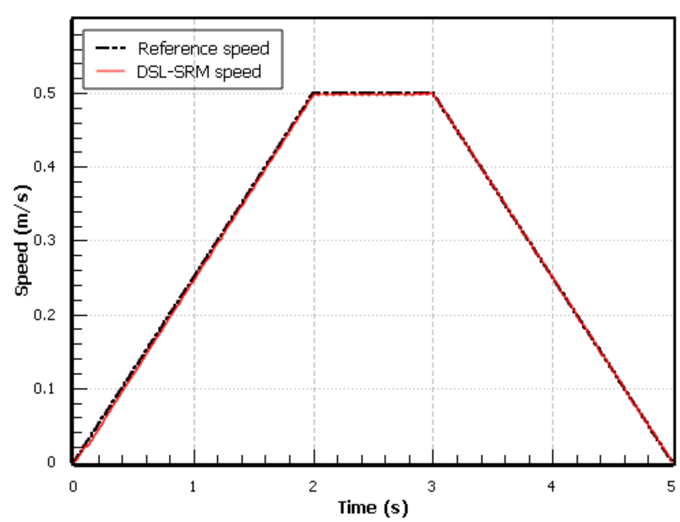

Fig. 10. Reference speed profile and actual DSL-SRM speed

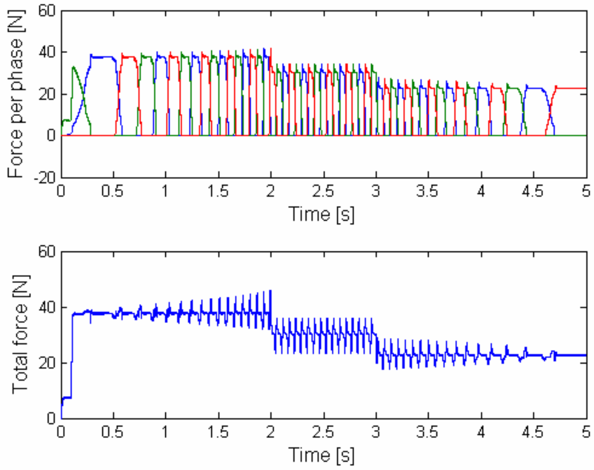

Fig. 11. Tangential force time, per each phases and total force

In the dynamic SIMULINK model, all the inductances and back **emf** values are implemented using the analytical model presented in the paper. For the tangential force look-up tables have been used, in order to obtain a more realistic profile, although the analytical model can be used too, as it gives a proper maximum force and a close pattern to that given by 2D-FEM, Fig. 5.

Fig. 11 displays the tangential forces during the simulation. It can be seen that the force ripple increases with speed and the average force value is the highest in the acceleration region and the lowest in the deceleration region.

The system modeled is particularly useful for adjusting the ON/OFF turn angles of the SRM phases, checking the limit speed that can be reached as well as the maximum attainable acceleration, among others.

VII. Conclusions

A double sided modular linear switched reluctance motor, with one mover and practically zero attraction force, is considered. Despite its quite large demand for reactive power, the DSL-SRM is an attractive alternative for low or high speed mass transfer drive systems.

In the paper, an attempt to an analytical development for DSP-SRM drive control is made. Two analytical models are developed for the considered linear motor. One model is based on the air-gap variable equivalent permeance concept. Within the second model, the motor phase flux linkage is described via a Fourier series with only two terms. The models' equivalence is proved too.

Three cases, concerning the way the phase coils are supplied are considered.

i) Both modules coils of a three phase double module motor are fed
ii) Only one coil of a three phase double module motor is fed
iii) The only phase coil of a three phase single module motor is fed.

The phase fluxes are calculated in the last two cases since the first case there are no fluxes in the air-gap from the un-energized phases. The DSL-SRM designed sample dynamic behavior, in the case of both modules coils supplied, are studied. The conclusions that came out of the presented study are:

i) The analytical models developed for DSL-SEM describe adequately the motor behavior, as seen from the comparison between the analytic calculated values and that obtained via 2D-FEM analysis.
ii) A control strategy can be developed based on analytical obtained results but it covers only partially the phenomenon, due to the important core saturation
iii) The SIMULINK program built on the analytic model can be a very useful tool in checking different control strategies.

It should be also pointed out the fact that the entire development presented for DSL-SRM can be easily applied to other similar motors with few changes.

References

[1] R.,Krishnan, *Switched reluctance motor drives*, CRC Press, London 2001.
[2] I.,Boldea, S.A.,Nasar,, *Linear electric actuators and generators*, Cambridge Univ. press, U.K., 1977
[3] F.,Daldaban, N.,Ustkoyuncu, "Analysis of a new double sided linear switched reluctance motor", Erciyes Univ. Journal, Turkey, vol 22, no. 1-2, pp 50-56, 2006
[4] U.S.,Deshpande, J.J.,Cathey, Richter, E., "A high force density linear switched reluctance machine", IEEE Trans on I.A., vol 31, no. 2, pp. 345-352, 1995
[5] C.T.,Liu, J.L.,Kuo, "Experimental investigation and 3D modeling of linear variable reluctance machine with magnetic-flux decoupled windings",IEEE Trans on Magnetics,vol.30,pp.4737-4739,Nov 1994.
[6] I.-A.,Viorel, L.,Szabo, Z.,Kovacs, "On the switched reluctance linear motor positioning system control", in Proc of PCIM, vol. Intelligent Motion, pp.477-484, 1998
[7] H.K.,Bae, B.S.,Lee, P.,Vijayraghavan, R.,Krishnan, "A linear switched reluctance motor: converter and control" IEEE Trans on IA., vol 36, no 5, pp. 1351-1359, 2000
[8] W.C.,Gan, N.C.,Cheung, L.,Qin, "Position control of linear switched reluctance motors for high precision applications", IEE Trans on IA, vol 39, no 5, pp 1350-1362, 2003
[9] I.-A.,Viorel, L.,Szabo, *Hybrid linear stepper motors*, Mediamira Publishing Company, Cluj, Romania, 1998
[10] G.Henneberger and I.A.Viorel, *Variable reluctance electrical machines*, Shaker Verlag, Aachen, Germany, 2001
[11] J.H.,Chang, D.H.,Kang, I.-A.,Viorel, Tomescu Ilinca, Strete Larisa, "Saturated Double Salient Reluctance Motors", in Proc. of ICEM 2006, Greece, on CD-ROM Summary PTA2-12, pp.530
[12] J.H.,Chang, D.H.,Kang,, I.-A.,Viorel, Strete Larisa, "Transverse flux reluctance linear motor's analytical model based on finite element method analysis results", IEEE Trans on Magnetics, vol 43, no 4, pp 1201-1204, 2007
[13] S.C.Chapra and R.P.Canale, *Numerical Methods for Engineers* (Third edition) McGraw-Hill Company, 1998
[14] H.-P.Chi, R.-L.Lin and J.F.Chen: "Simplified flux-linkage model for switched reluctance motors", IEE Proc. Electr. Power Appl., vol.152, no.3, pp.577-583, 200